Sprite beads originating from inhomogeneities in the mesospheric electron density

A. Luque[1] and F. J. Gordillo-Vázquez[1]

Received 4 December 2010; revised 18 January 2011; accepted 19 January 2011; published 25 February 2011.

[1] Small, persistent luminous spots observed in sprites may be originated by underlying inhomogeneities in the density of free electrons. Using a streamer density model, we show that the collision of a streamer with a localized enhancement of ionization leaves a region of reduced conductivity and enhanced field in the streamer channel. We discuss the light emissions from this region and predict its spectrum. These emissions are identified with "sprite beads" and we propose that they may serve to investigate the spatial distribution of free electrons in the upper atmosphere above a thunderstorm. **Citation:** Luque, A., and F. J. Gordillo-Vázquez (2011), Sprite beads originating from inhomogeneities in the mesospheric electron density, *Geophys. Res. Lett.*, *38*, L04808, doi:10.1029/2010GL046403.

1. Introduction

[2] Sprites are transient luminous events (TLE) observed in the mesosphere, triggered by a lightning stroke from a thunderstorm (see the recent reviews by *Pasko* [2010], *Inan et al.* [2010] and *Ebert et al.* [2010]). Since they were first observed by *Franz et al.* [1990], sprites have attracted a large community of researchers from the geosciences. An often quoted reason for this interest is that the mesosphere is one of the least understood layers of the Earth's atmosphere, being too rarefied to sustain an aircraft but still offering too much drag to a satellite. The scarcity of in-situ measurements can be palliated in part by sprites and related TLE's, which reveal in their emissions details of the mesosphere during thunderstorms.

[3] Consider, for example, the density and spatial distribution of free electrons –a relevant ingredient in the physics of the mesosphere. In this letter we investigate how small, localized enhancements of this density produce, after the passage of a sprite streamer, persistent optical emissions that we identify with sprite beads.

[4] The term "sprite bead" was coined by *Sentman et al.* [1996] for bright, standing spots in the filamentary (streamer) region of sprites with lifetimes of about 100 ms but sometimes lasting up to a second [*Stenbaek-Nielsen and McHarg*, 2008]. These structures appear frequently in sprite images; they have also been analyzed by *Stenbaek-Nielsen et al.* [2000], *Moudry et al.* [2003], *Gerken and Inan* [2002, 2003] and *Marshall and Inan* [2006]. *Stenbaek-Nielsen and McHarg* [2008] and *Stenbaek-Nielsen et al.* [2000] reported that beads are often starting points for later sprites, re-ignited by the subsequent activity of the thunderstorm tens or hundreds of milliseconds after the emissions from the initial sprite have decayed. In some observations, beads move slowly upwards [*Gerken and Inan*, 2002; *Stenbaek-Nielsen and McHarg*, 2008] but they seem to be mostly stationary [*Marshall and Inan*, 2006].

[5] Presently there is no widely accepted model of sprite beads. *Stenbaek-Nielsen et al.* [2000] pointed to a chemical origin because at that time it was thought that electric fields could not persist in the mesosphere during the full lifetime of the beads. However, *Hu et al.* [2007] measured continuing currents from thunderstrokes lasting hundreds of milliseconds that cause long-lasting electrostatic fields at high altitude.

[6] Here we show simulations of beads arising from the passage of a downward, positive sprite streamer through a local enhancement of the density of free electrons. After 2 ms of simulation time, the streamer branches –this is roughly consistent with observations; reliable simulations lasting longer than this time would require a fully 3D model presently not available. Within this constraint we reproduce many of the features of sprite beads at short timescales. We therefore suggest that sprite beads may serve as a proxy to study the spatial distribution of free electrons in the mesosphere above a thundercloud.

2. Model

[7] We use the density model of *Luque and Ebert* [2009, 2010], where electrons diffuse and drift in the local electric field with an altitude-dependent mobility. Electron-ion pairs are created by impact ionization and photo-ionization; dissociative attachment to O_2 removes free electrons. The rates of these reactions depend on the air density and thus on altitude. The partial differential equations that we are solving and the parametrization that we use are detailed in the supplementary material of *Luque and Ebert* [2009].

[8] The altitude profile of free electron density in the mesosphere at the moment of sprite inception is at present very uncertain. Numerical models [*Pasko et al.*, 1997; *Marshall et al.*, 2008; *Luque and Ebert*, 2009] consistently show a significant depletion of electrons due to dissociative attachment enhanced by electric fields below the breakdown threshold, E_k. In the numerical simulations by *Luque and Ebert* [2009] a sharp front emerges that separates electron densities that differ by a factor $\sim 10^5$ across a distance of about 1 km. Based on this, the initial electron density of *Luque and Ebert* [2010] that we also use here is a sharp step located at 85 km, where we neglect the ionization below this altitude and set the upper ionization to 90 cm^{-3}, electrically neutral everywhere.

[9] Other parameters of the simulation of *Luque and Ebert* [2010] are also reproduced here: we simulate a cylindrical

[1]Instituto de Astrofísica de Andalucía, CSIC, Granada, Spain.

0094-8276/11/2010GL046403

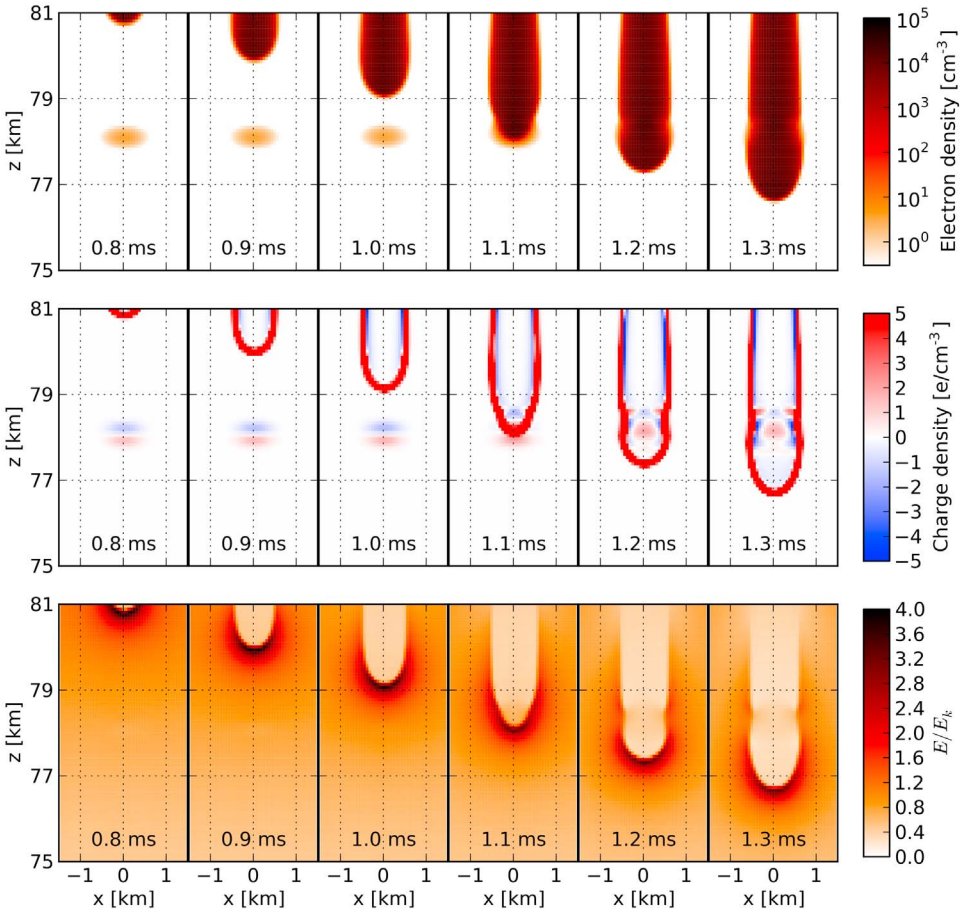

Figure 1. Collision between a downward, positive sprite streamer and a patch of locally enhanced ionization (ionization bump). Shown are the electron density in logarithmic scale, the space charge density in a scale truncated to emphasize the charge structure around the bump and the reduced electric field E/E_k. A schematic view of this collision is shown in Figure 2.

volume with altitudes from 65 km to 90 km and a radius of 25 km. The simulation assumes a perfect cylindrical symmetry and has a highest spatial resolution of 2.4 m both in the radial and in the axial direction. For simplicity, we assume a homogeneous and constant electric field of 40 V/m. According to our parameters this field exceeds E_k above approximately 81.3 km.

[10] A streamer is initiated by a gaussian ionization seed in the steep front at 85 km, with a width of 200 m and a highest density of 90 electron-ion pairs per cm^3. A second gaussian, electrically neutral bump in the ionization is placed directly below the streamer with electron and ion densities both equal to $n_{bump} = A \exp(-(z-H)^2/W_z^2 - r^2/W_r^2)$. We investigated the effect of this second bump depending on its parameters: we kept a constant vertical width $W_z = 185$ m and altitude $H = 78$ km but we varied the horizontal width W_r between 185 and 492 m and the peak density A from $7 \cdot 10^{-1}$ and $7 \cdot 10^2$.

3. Results

3.1. Streamer-Bump Collision

[11] Figure 1 shows the head-on collision of a sprite streamer with an electron density bump at 78 km altitude, with a width $W_r = 370.3$ m and highest electron density $A = 65.2$ cm^{-3}. We note the following features, present in all our simulations:

[12] 1. At the moment of the streamer-bump collision (about 1.1 ms), the electric field at the streamer head decreases slightly, due to the higher conductivity created by the enhanced electron density in the bump. Later, the electric field in the streamer tip recovers its original value but there is a persistent enhancement of the electric field at the altitude of the original bump. At 1.3 ms this electric field is $E \approx 0.8E_k$.

[13] 2. Even though the highest electron density in the bump is much smaller than the electron density in the streamer (in Figure 1 it is about three orders of magnitude smaller), it causes a significant and lasting effect in the streamer channel. At the latest time in Figure 1 (1.3 ms), the channel is distinctly thinner at the location of the initial bump.

[14] 3. The collision causes a relatively complex and lasting structure in the space charge inside the streamer channel. This is related to the thinning of the streamer channel and it is the cause of the persistent enhanced electric field.

[15] 4. The propagating speed of the streamer head is barely affected by the presence of the ionization bump. Only around the collision time the streamer head speed jumps slightly as it absorbs the ionization bump.

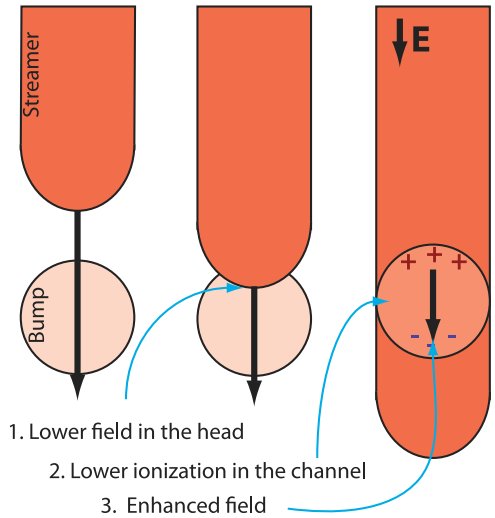

Figure 2. Scheme of a streamer-bump collision. A higher local air conductivity in the ionization bump defocuses the electric field in the streamer tip. The result is a hole (or "bubble") in the streamer channel. Finally, since electrons are still drifting upwards inside the channel, they create a charge separation that enhances the field inside the bubble. Note that a locally increased conductivity screens the electric field inside, whereas a locally depleted conductivity enhances it.

[16] The overall mechanism of streamer-bump collision is summarized in Figure 2. As the streamer head goes through the ionization bump, the increased local conductivity of the air reduces the driving electric field at the streamer tip. This in turn decreases the electron multiplication rate in such a manner that, even though at that area the initial electron density was higher, after the passage of the streamer head there remains a volume of lower ionization in the streamer body (a kind of ionization "bubble"). Since the electric field is not fully screened inside the streamer, electrons continue to drift upwards and the upper side of the bubble is charged positively, while the lower side is charged negatively. This is the source of a localized and persistent enhancement of the electric field.

3.2. Luminosity

[17] Figure 3a shows the evolution of the optical emissions from the same simulation as Figure 1. Here we used the model developed by *Pasko et al.* [1997] to calculate the emissions in the first positive system of N_2. These emissions dominate ground-based sprite observations.

[18] The emissions in Figure 3a exhibit some of the features that have already been discussed by *Luque and Ebert* [2010]: namely the exponential increase in light emissions from the streamer head and the trailing emissions visible in the upper boundary of our picture (explained also by *Liu* [2010]; called "afterglow" by *Morrill et al.* [1998]; *Bucsela et al.* [2003]; *Kanmae et al.* [2007] and *Sentman et al.* [2008]). Here we focus on the effect of the electron bump at 78 km, whose most prominent effect is the persistent optical emission that lasts until the end of our simulation.

[19] In Figure 3a the emissions from the sprite bead reach about 10^6 R (1 R (Rayleigh) = 10^6 photons/cm^{2}s) but this value depends strongly on the initial conditions of the ionization bump. Figure 3b shows the highest emission rates for beads generated from different bumps. We obtained intensities between 10^5 R and 10^7 R for widths W_r between 185 m and 617 m and peak ionization densities A between about 1 cm^{-3} and 10^3 cm^{-3}. The luminosity increases with increasing A and decreasing W_r. For high ionizations the luminosity does not depend on the size of the bump because the streamer is so strongly perturbed that one should rather view it as a new streamer emerging from the bump; then the width of the bump is not very relevant. In the following section we will see also that high densities in the bump destabilize the streamer front; this is why the dependence in Figure 3b is irregular for high A.

[20] Note that in Figure 3a the sprite bead emerges at its full luminosity immediately after the passage of the streamer head, while in the high-speed observations of *Stenbaek-Nielsen and McHarg* [2008] the bead is delayed some tenths of a millisecond. The cause of this discrepancy may be that we used high ionization bumps in order to obtain visible emissions within the time constraint of our simulations. Presently we are unable to apply our numerical model to weaker bumps and test if they would produce delayed visible emissions. Also, for longer time-scales, slower chemical processes not included in our model may be relevant.

3.3. Destabilization of the Streamer Front

[21] When the density in the ionization bump is high enough, it can significantly affect the propagation of the streamer. In many of our simulations the streamer branches shortly after passing through the ionization bump. Since our simulations were restricted to cylindrically symmetrical streamers, here "branching" is interpreted as a losing of the convexity in the streamer head (for a discussion about this concept and its close relationship to actual 3D branching, see A. Luque and U. Ebert (Density models for streamer discharges: Beyond cylindrical symmetry and homogeneous media, submitted to *Journal of Computational Physics*, 2010).

[22] *Stenbaek-Nielsen and McHarg* [2008] observed that sprite beads are often associated with sprite streamer branching. Our simulations show that a large ionization bump causes both a luminous bead and streamer branching. This is perhaps not the only reason for the connection between these two phenomena: the electric field is also locally enhanced in the irregular geometry of a forked channel and this could also explain persistent emissions at a branching point. Nevertheless, sprite streamers show branching patterns not observed in the laboratory, such as the splitting into more than two streamers observed by *McHarg et al.* [2010]. It is thus reasonable to speculate that additional mechanisms for streamer branching are at play at high altitudes that are not present in laboratory discharges.

3.4. Predicted Spectra of Sprite Beads

[23] In Figure 3c we show a predicted spectrum of the emissions from a sprite bead according to our model and the sprite kinetic model of *Gordillo-Vázquez* [2008, 2010]. From the simulation of Figures 1 and 3a, we extracted the time-dependent electric field in the streamer-bead axis at 78 km and used it as an input to the zero-dimensional kinetic model. The emissions are integrated in time starting at the passage of the streamer head (1.2 ms) and up to 2 ms, that is, the plotted intensities do not include emissions from the

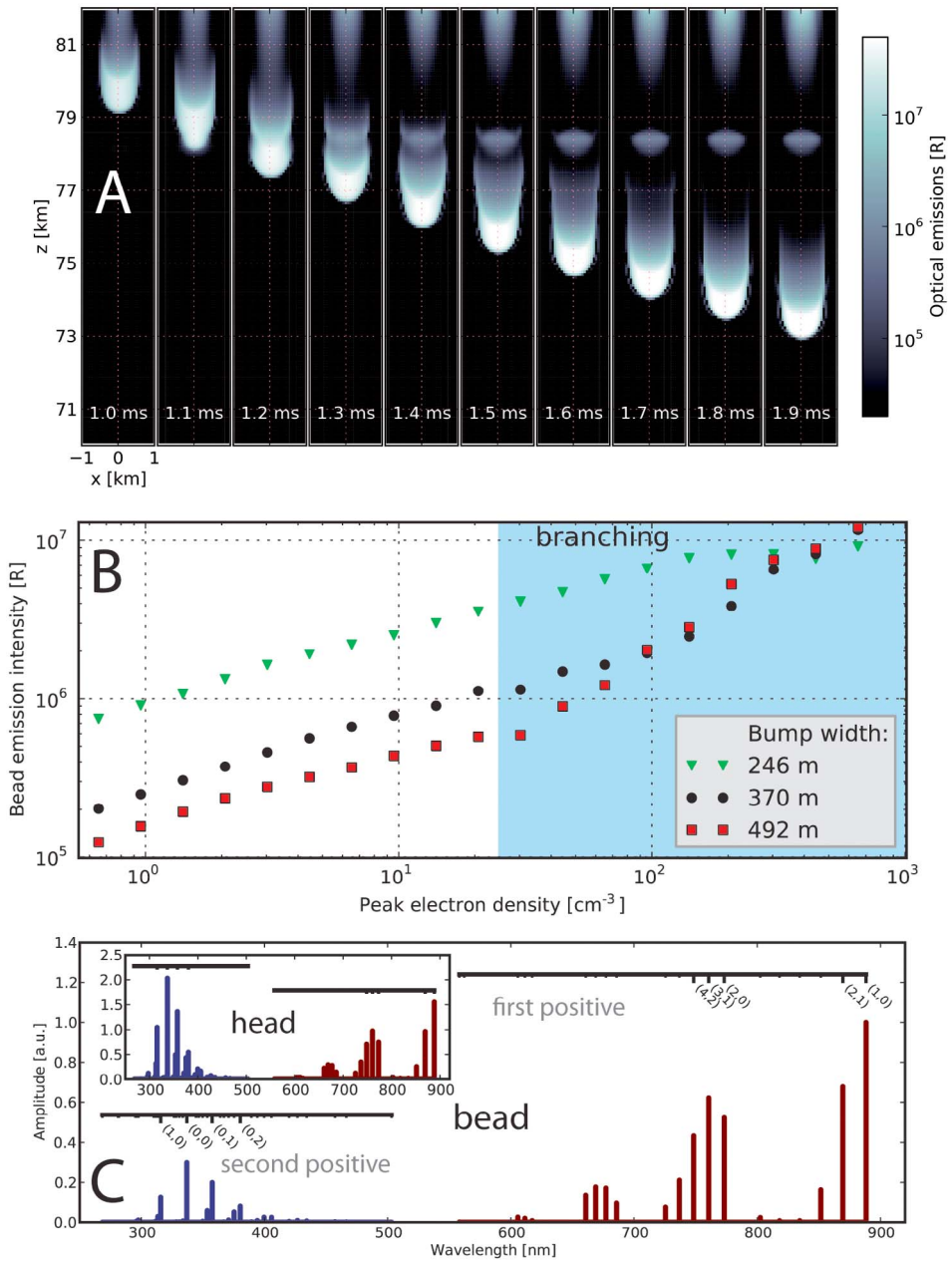

Figure 3. (a) Light emissions in the first positive system of N_2 for a streamer and a bead at 78 km. We plot emissions averaged over an exposure time of 0.1 ms; since the streamer heads moves quickly while the bead stands still, this averaging reduces the ratio of the relative intensities between streamer and bead. The emissions are integrated along a horizontal line-of-sight (i.e., Abel-transformed) and expressed in Rayleigh (R). (b) Emission intensity from a sprite bead depending on the width and the amplitude of the ionization bump. The shaded area to the right indicates that when the peak density in the bump is high enough the streamer is destabilized and often branches. The streamer did not branch in all the simulations in the shaded area, but it did in a majority of them and in none of the simulations with lower densities. (c) Simulated spectrum of the bead shown in Figure 3a and spectrum of a sprite streamer head at the same altitude (inset). We have labelled the most important emissions (v', v'') for the first positive system (red; right) $N_2(B^3\Pi_g, v') \rightarrow N_2(A^3\Sigma_u^+, v'')$ and the second positive (blue; left) $N_2(C^3\Pi_u, v') \rightarrow N_2(B^3\Pi_g, v'')$. Both the bead and the head spectra are normalized to the (1, 0) line of the first positive system in the bead spectrum; intensities are therefore comparable between all spectra.

head. Bead spectroscopy could be carried out with cameras coupled to spectrographs covering the 300 nm–400 nm and 600 nm–800 nm spectral ranges to record spectral features of the N_2 second and first positive systems, respectively.

[24] Our spectrum also shows near infrared (NIR) emissions, namely the (2,1) and (1,0) transitions corresponding, respectively, to 869.50 nm and 888.30 nm, the latter being the strongest line emissions within the first positive system

of N_2. *Siefring et al.* [2010] recently published observations of sprites in this spectral range.

[25] The inset in Figure 3c shows the spectrum of the streamer head from the same simulation (i.e., emissions integrated up to 1.2 ms). The most outstanding difference between the two spectra is the variation in the relative intensities of the first and second positive systems. The streamer head is associated with higher reduced electric fields and hence more energetic electrons that excite more efficiently the $N_2(C^3\Pi_u)$ electronic state that emits in the blue.

4. Conclusions

[26] Besides providing a plausible explanation for widely observed sprite beads, our result suggests that the optical observation of sprites may serve to investigate the spatial distribution of free electrons in the mesosphere above a thundercloud.

[27] Our simulations show that due to the strongly nonlinear nature of streamers, small inhomogeneities in the density of free electrons produce observable optical emissions after the passage of a sprite streamer. We lack a clear understanding on the origin of these inhomogeneities; possible sources are atmospheric turbulence [*Pfrommer et al.*, 2009], extensive showers generated by high-energy cosmic rays, meteor-induced ionization [*Gelinas et al.*, 1998] and pre-ionization caused by the electromagnetic pulse of a return stroke [*Valdivia et al.*, 1997]. We note that these inhomogeneities are always too weak to initiate streamers by their own; isolated patches of ionization would initiate double-headed streamers, propagating both upwards and downwards [*Liu and Pasko*, 2004], and these have never been observed [*Stenbaek-Nielsen and McHarg*, 2008].

[28] **Acknowledgments.** This work was supported by the Spanish Ministry of Science and Innovation, MICINN under project AYA2009-14027-C05-02 and by the Junta de Andalucía, Proyecto de Excelencia FQM-5965.

[29] W. K. Peterson thanks two anonymous reviewers.

References

Bucsela, E., J. Morrill, M. Heavner, C. Siefring, S. Berg, D. Hampton, D. Moudry, E. Wescott, and D. Sentman (2003), $N_2(B^3\Pi_g)$ and $N_2^+(A^2\Pi_u)$ vibrational distributions observed in sprites, *J. Atmos. Sol. Terr. Phys.*, *65*, 583, doi:10.1016/S1364-6826(02)00316-4.

Ebert, U., S. Nijdam, C. Li, A. Luque, T. Briels, and E. van Veldhuizen (2010), Review of recent results on streamer discharges and discussion of their relevance for sprites and lightning, *J. Geophys. Res.*, *115*, A00E43, doi:10.1029/2009JA014867.

Franz, R. C., R. J. Nemzek, and J. R. Winckler (1990), Television image of a large upward electrical discharge above a thunderstorm system, *Science*, *249*, 48, doi:10.1126/science.249.4964.48.

Gelinas, L. J., K. A. Lynch, M. C. Kelley, S. Collins, S. Baker, Q. Zhou, and J. S. Friedman (1998), First observation of meteoritic charged dust in the tropical mesosphere, *Geophys. Res. Lett.*, *25*, 4047, doi:10.1029/1998GL900089.

Gerken, E. A., and U. S. Inan (2002), A survey of streamer and diffuse glow dynamics observed in sprites using telescopic imagery, *J. Geophys. Res.*, *107*(A11), 1344, doi:10.1029/2002JA009248.

Gerken, E. A., and U. S. Inan (2003), Observations of decameter-scale morphologies in sprites, *J. Atmos. Sol. Terr. Phys.*, *65*, 567, doi:10.1016/S1364-6826(02)00333-4.

Gordillo-Vázquez, F. J. (2008), Air plasma kinetics under the influence of sprites, *J. Phys. D*, *41*(23), 234016, doi:10.1088/0022-3727/41/23/234016.

Gordillo-Vázquez, F. J. (2010), Vibrational kinetics of air plasmas induced by sprites, *J. Geophys. Res.*, *115*, A00E25, doi:10.1029/2009JA014688.

Hu, W., S. A. Cummer, and W. A. Lyons (2007), Testing sprite initiation theory using lightning measurements and modeled electromagnetic fields, *J. Geophys. Res.*, *112*, D13115, doi:10.1029/2006JD007939.

Inan, U. S., S. A. Cummer, and R. A. Marshall (2010), A survey of ELF and VLF research on lightning-ionosphere interactions and causative discharges, *J. Geophys. Res.*, *115*, A00E36, doi:10.1029/2009JA014775.

Kanmae, T., H. C. Stenbaek-Nielsen, and M. G. McHarg (2007), Altitude resolved sprite spectra with 3 ms temporal resolution, *Geophys. Res. Lett.*, *34*, L07810, doi:10.1029/2006GL028608.

Liu, N. (2010), Model of sprite luminous trail caused by increasing streamer current, *Geophys. Res. Lett.*, *37*, L04102, doi:10.1029/2009GL042214.

Liu, N., and V. P. Pasko (2004), Effects of photoionization on propagation and branching of positive and negative streamers in sprites, *J. Geophys. Res.*, *109*, A04301, doi:10.1029/2003JA010064.

Luque, A., and U. Ebert (2009), Emergence of sprite streamers from screening-ionization waves in the lower ionosphere, *Nat. Geosci.*, *2*, 757, doi:10.1038/ngeo662.

Luque, A., and U. Ebert (2010), Sprites in varying air density: Charge conservation, glowing negative trails and changing velocity, *Geophys. Res. Lett.*, *37*, L06806, doi:10.1029/2009GL041982.

Marshall, R. A., and U. S. Inan (2006), High-speed measurements of small-scale features in sprites: Sizes and lifetimes, *Radio Sci.*, *41*, RS6S43, doi:10.1029/2005RS003353.

Marshall, R. A., U. S. Inan, and T. W. Chevalier (2008), Early VLF perturbations caused by lightning EMP-driven dissociative attachment, *Geophys. Res. Lett.*, *35*, L21807, doi:10.1029/2008GL035358.

McHarg, M. G., H. C. Stenbaek-Nielsen, T. Kanmae, and R. K. Haaland (2010), Streamer tip splitting in sprites, *J. Geophys. Res.*, *115*, A00E53, doi:10.1029/2009JA014850.

Morrill, J. S., E. J. Bucsela, V. P. Pasko, S. L. Berg, M. J. Heavner, D. R. Moudry, W. M. Benesch, E. M. Wescott, and D. D. Sentman (1998), Time resolved N2 triplet state vibrational populations and emissions associated with red sprites, *J. Atmos. Sol. Terr. Phys.*, *60*, 811, doi:10.1016/S1364-6826(98)00031-5.

Moudry, D., H. Stenbaek-Nielsen, D. Sentman, and E. Wescott (2003), Imaging of elves, halos and sprite initiation at 1ms time resolution, *J. Atmos. Sol. Terr. Phys.*, *65*, 509, doi:10.1016/S1364-6826(02)00323-1.

Pasko, V. P. (2010), Recent advances in theory of transient luminous events, *J. Geophys. Res.*, *115*, A00E35, doi:10.1029/2009JA014860.

Pasko, V. P., U. S. Inan, T. F. Bell, and Y. N. Taranenko (1997), Sprites produced by quasi-electrostatic heating and ionization in the lower ionosphere, *J. Geophys. Res.*, *102*, 4529, doi:10.1029/96JA03528.

Pfrommer, T., P. Hickson, and C.-Y. She (2009), A large-aperture sodium fluorescence lidar with very high resolution for mesopause dynamics and adaptive optics studies, *Geophys. Res. Lett.*, *36*, L15831, doi:10.1029/2009GL038802.

Sentman, D. D., E. M. Wescott, M. Heavner, and D. Moudry (1996), Observations of sprite beads and balls, *Eos Trans. AGU*, *77*, F61.

Sentman, D. D., H. C. Stenbaek-Nielsen, M. G. McHarg, and J. S. Morrill (2008), Plasma chemistry of sprite streamers, *J. Geophys. Res.*, *113*, D11112, doi:10.1029/2007JD008941.

Siefring, C. L., J. S. Morrill, D. D. Sentman, and M. J. Heavner (2010), Simultaneous near-infrared and visible observations of sprites and acoustic-gravity waves during the EXL98 campaign, *J. Geophys. Res.*, *115*, A00E57, doi:10.1029/2009JA014862.

Stenbaek-Nielsen, H. C., and M. G. McHarg (2008), High time-resolution sprite imaging: Observations and implications, *J. Phys. D*, *41*(23), 234009, doi:10.1088/0022-3727/41/23/234009.

Stenbaek-Nielsen, H. C., D. R. Moudry, E. M. Wescott, D. D. Sentman, and F. T. S. Sabbas (2000), Sprites and possible mesospheric effects, *Geophys. Res. Lett.*, *27*, 3829, doi:10.1029/2000GL003827.

Valdivia, J. A., G. Milikh, and K. Papadopoulos (1997), Red sprites: Lightning as a fractal antenna, *Geophys. Res. Lett.*, *24*, 3169, doi:10.1029/97GL03188.

F. J. Gordillo-Vázquez and A. Luque, Instituto de Astrofísica de Andalucía, CSIC, PO Box 3004, E-18080 Granada, Spain. (vazquez@iaa.es; aluque@iaa.es)